

Synthesis and Antiproliferative Activity of New Ruthenium Complexes with Ethacrynic Acid-Modified Pyridine- and Triphenylphosphine- Ligands

Gabriele Agonigi,^a Tina Riedel,^b Stefano Zacchini,^c Emilia Păunescu,^b Guido Pampaloni,^a Niccolò Bartalucci,^a Paul J. Dyson,^{b,} Fabio Marchetti^{a,*}*

^a Dipartimento di Chimica e Chimica Industriale, Università di Pisa, Via G. Moruzzi 13, I-56124 Pisa, Italy;

^bInstitut des Sciences et Ingénierie Chimiques, Ecole Polytechnique Fédérale de Lausanne (EPFL), CH-1015 Lausanne, Switzerland;

^cDipartimento di Chimica Industriale “Toso Montanari”, Università di Bologna, Viale Risorgimento 4, I-40136 Bologna, Italy.

Abstract

Pyridine- and phosphine-based ligands modified with ethacrynic acid (a broad acting glutathione transferase inhibitor) were prepared and coordinated to ruthenium(II)-arene complexes and to a ruthenium(III) NAMI-A type complex. All the compounds (ligands and complexes) were fully characterized by analytical and spectroscopic methods and, in one case, by single-crystal X-ray diffraction. The *in vitro* anticancer activity of the compounds was studied, with the compounds displaying moderate cytotoxicity toward the human ovarian cancer cell lines. All the complexes led to similar levels of residual GST activity in the different cell lines, irrespective of the stability of the Ru-ligand bond.

Keywords: bioorganometallic chemistry, bioinorganic chemistry, metal-based drugs, ruthenium complexes, ethacrynic acid

Introduction

There are currently considerable ongoing research efforts to develop new, efficient metal-based anticancer agents that overcome the limitations associated with platinum-based drugs.¹ In this context, ruthenium-based complexes have aroused great interest and two of them, *i.e.* [indazoleH][*trans*-Ru(*N*-indazole)₂Cl₄] (KP1019) and [imidazoleH][*trans*-Ru(*N*-imidazole)(*S*-dmsO)Cl₄] (NAMI-A), have entered phase II of clinical trials (Figure 1).² It is believed that KP1019 and NAMI-A are pro-drugs, being converted into more active Ru(II) species in the tumor environment.³ In part, this feature has triggered studies on ruthenium(II) complexes, especially those based on the [Ru(η^6 -arene)Cl₂] frame.⁴ In this respect, complexes containing 1,3,5-triaza-7-phosphatricyclo[3.3.1.1]decane (PTA, affording RAPTA complexes – Figure 1) and ethylene-1,2-diamine as ligands have emerged as among the most promising species, showing relevant antitumor properties *in vivo*.⁵

In addition to these non-targeted compounds, i.e. compounds that were not designed to interfere with specific targets overexpressed or uniquely expressed in cancer cells, the synthesis of metal complexes containing organic fragments with known biological functions can lead to enhanced anticancer activities.⁶ In this context, the ruthenium(II)-arene structure has been modified with various bioactive groups, usually via the inclusion of a functional ligand or via modification of the η^6 -coordinated arene ligand with an appropriate functional moiety.⁷ For example, 3-hydroxyflavones,⁸ lapachol,⁹ paullones,¹⁰ and lonidamine,¹¹ each with a well-characterized biological (anticancer) property, have been directly coordinated to the ruthenium(II)-arene fragment. Of the different biologically active groups used, ethacrynic acid (EA-CO₂H), an effective inhibitor of glutathione transferases (GSTs), which comprises a family of cytosolic detoxification enzymes associated with drug resistance in primary and metastatic tumors,¹² has been tethered to the ruthenium(II)-arene unit via both the arene ligand¹² and via imidazole-modified co-ligands.¹³ Furthermore, platinum(IV) complexes have also been modified with ethacrynic acid.¹⁴ These complexes have been shown to inactivate GSTs and induce apoptosis even in cisplatin resistant cell lines.¹⁵

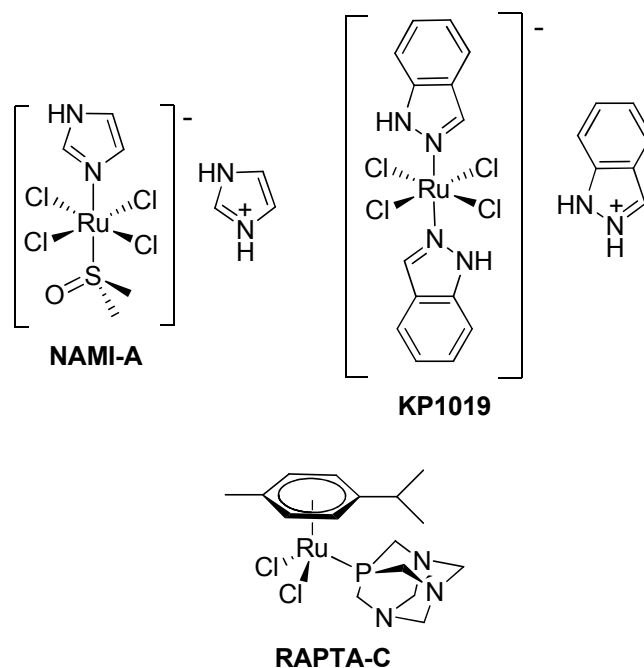
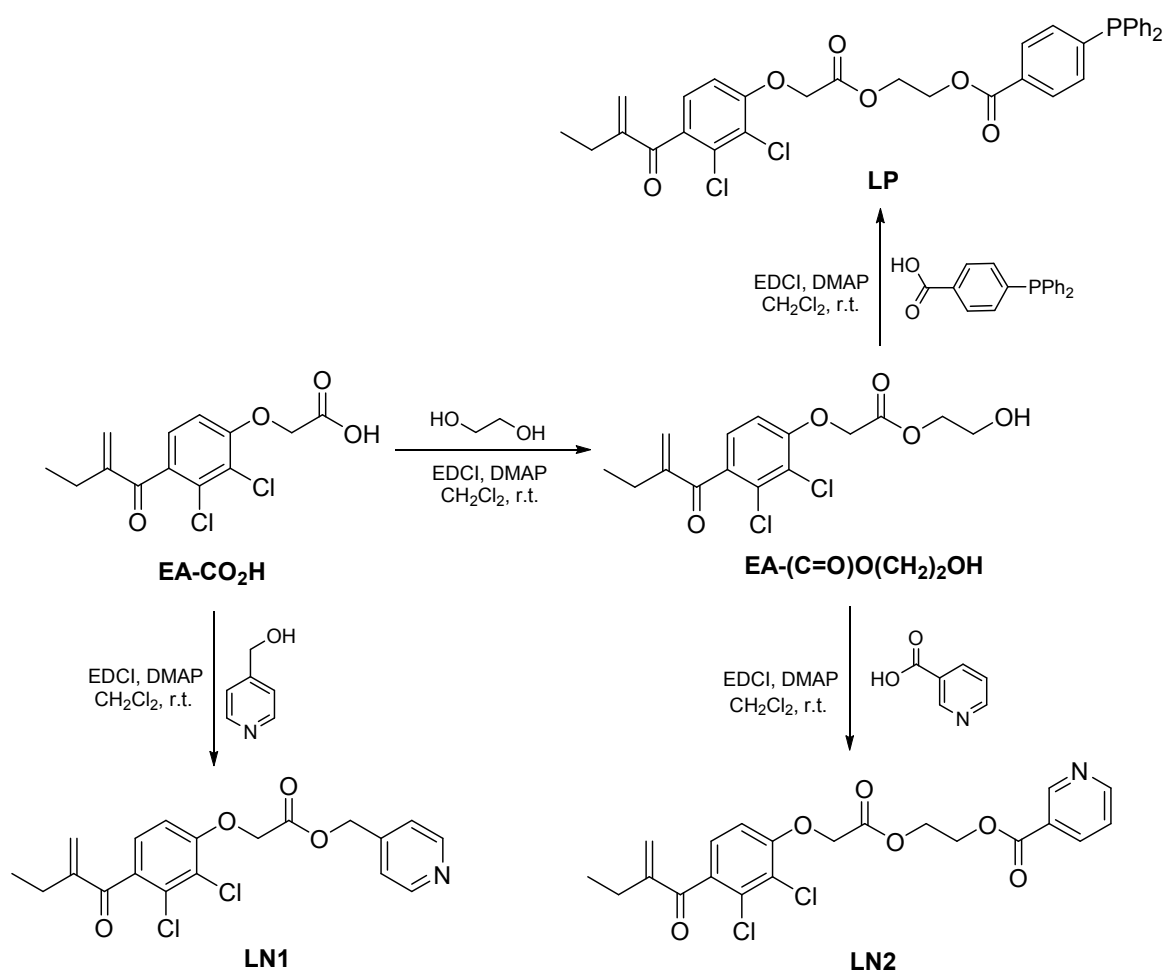


Figure 1. Structures of ruthenium complexes with known antitumor activity.

In the present study, new EA-CO₂H functionalized N- and P-donor ligands are described, together with their coordination to ruthenium(II)-arene and ruthenium(III) NAMI-A-like complexes. The antiproliferative properties of all the compounds were explored.

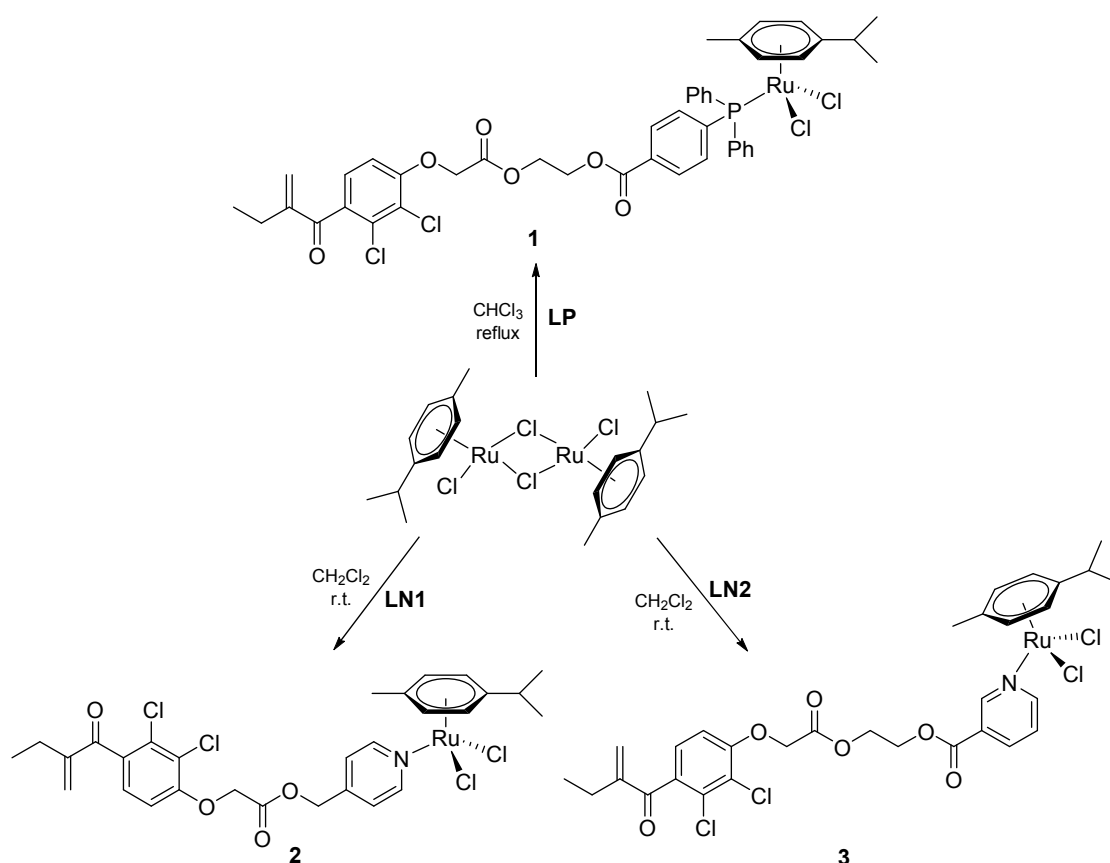
Results and discussion

Three ethacrynic acid-functionalized ligands were prepared from the reaction of EA-CO₂H with 4-(diphenylphosphino)benzoic acid, 4-pyridinemethanol or nicotinic acid (Scheme 1). Thus **LN1** was obtained in 77% yield from EA-CO₂H and 4-pyridinemethanol via a EDCI/DMAP-mediated coupling reaction. The synthesis of **LN2** and **LP** required initial derivatization of ethacrynic acid into the alcohol EA-(C=O)O(CH₂)₂OH. This underwent EDCI/DMAP-mediated coupling reactions with nicotinic acid and 4-(diphenylphosphino)benzoic acid to give **LN2** (81% yield) and **LP** (62% yield), respectively. EA-(C=O)O(CH₂)₂OH, **LN1**, **LN2** and **LP** were purified by silica chromatography, isolated as solid materials and then characterized by means of analytical and spectroscopic techniques. EA-(C=O)O(CH₂)₂OH, **LP** and **LN2** were found to be room temperature stable, whereas **LN1** required low temperature storage.



Scheme 1. Synthesis of *N*- and *P*-donor ligands from ethacrynic acid (EA-CO₂H).

The reaction of $[(\eta^6\text{-}p\text{-cymene})\text{RuCl}_2]_2$ with **LP** in chloroform under reflux afforded **1**, which was isolated in 60% yield after work up. Complexes **2** - **3** were obtained in *ca.* 75% yield by reaction of $[(\eta^6\text{-}p\text{-cymene})\text{RuCl}_2]_2$ with the appropriate pyridine ligand, **LN1** or **LN2**, in dichloromethane at room temperature (Scheme 2).



Scheme 2. Preparation of the ruthenium(II)-*p*-cymene complexes **1** - **3** containing ethacrynic acid-functionalized ligands.

Complexes **1** - **3** are air-stable in the solid state and in solution and are soluble in common organic solvents, but insoluble in water. The IR spectra of **1** - **3** (similar to the spectra of **LP**, **LN1** and **LN2**) display absorptions in the range $1764\text{-}1661\text{ cm}^{-1}$, attributable to the stretching vibrations of the carbonyl and alkene moieties. The ^1H and ^{13}C NMR spectra of **1** - **3** in CDCl_3 display the resonances due to EA-CO₂H very close in value to those previously reported for the same fragment.¹³ However, as a consequence of *N*-coordination, the ^1H and ^{13}C resonances related to the adjacent nuclei within the pyridyl moiety of **2** - **3** are shifted significantly downfield. More precisely, for the **3** - **LN2** pair a difference of $\Delta\delta_{\text{H}} \approx 0.4\text{ ppm}$ in the ^1H spectrum and $\Delta\delta_{\text{C}} \approx 5\text{ ppm}$ in the ^{13}C spectrum was observed. Analogously, the ^{31}P resonance of **LP** ($\delta_{\text{P}} = -4.9\text{ ppm}$) undergoes strong downfield shift in **1** ($\delta_{\text{P}} = 25.3$

ppm), as result of coordination to the ruthenium centre. The proposed structures were also confirmed by mass spectrometry analyses.

Single crystals of **2** suitable for X-ray diffraction analysis were obtained from a THF/hexane solution settled at $-30\text{ }^{\circ}\text{C}$. The molecular structure of **2** is shown in Figure 2 with key geometric parameters given in Table 1. Compound **2** adopts the characteristic three-leg piano-stool geometry previously found in several Ru(II)-arene complexes.¹⁶ The bonding parameters around the Ru(II) center are similar to those previously found in related complexes.^{13,17} The bonding parameters of the EA-CO₂H unit are not significantly different respect to other reported structures.^{12,13,18}

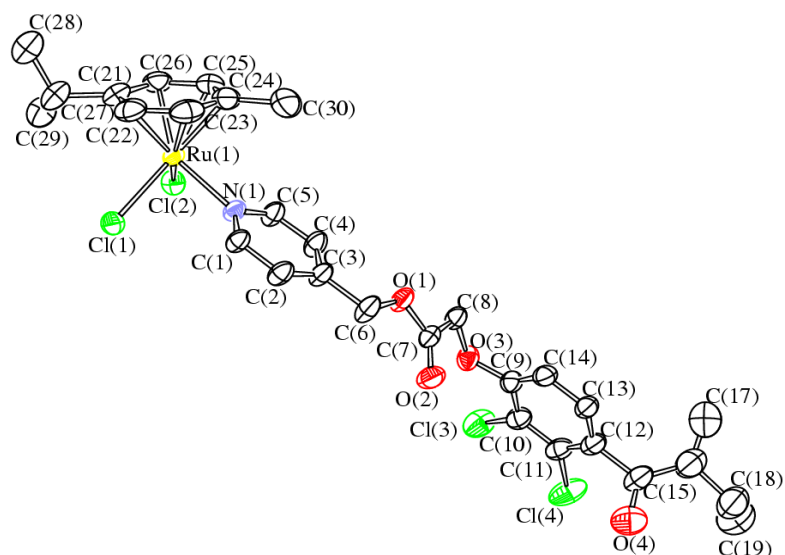


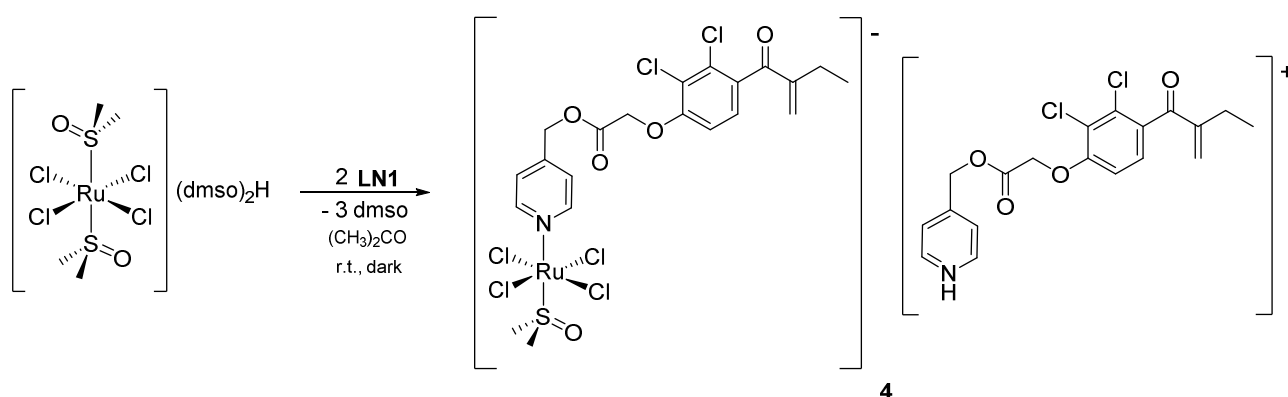
Figure 2. Molecular structure of Ru(η^6 -*p*-cymene)Cl₂(LN1), **2**. Displacement ellipsoids are at the 50% probability level.

Table 1. Selected bond distances (Å) and angles (°) for **2**.

Ru(1)-C(21)	2.180(4)	Ru(1)-C(22)	2.135(5)
Ru(1)-C(23)	2.139(5)	Ru(1)-C(24)	2.188(5)
Ru(1)-C(25)	2.177(4)	Ru(1)-C(26)	2.163(4)
Ru(1)-Cl(1)	2.4111(10)	Ru(1)-Cl(2)	2.4047(11)
Ru(1)-N(1)	2.133(3)	N(1)-C(1)	1.338(5)

N(1)-C(5)	1.341(5)	C(3)-C(6)	1.505(5)
C(6)-O(1)	1.441(5)	O(1)-C(7)	1.324(5)
C(7)-O(2)	1.183(5)	C(7)-C(8)	1.513(9)
C(8)-O(3)	1.429(9)	O(3)-C(9)	1.344(7)
Cl(1)-Ru(1)-Cl(2)	89.90(9)	Cl(1)-Ru(1)-N(1)	85.89(9)
Cl(2)-Ru(1)-N(1)	86.24(9)	C(3)-C(6)-O(1)	107.4(3)
C(6)-O(1)-C(7)	118.4(3)	O(1)-C(7)-O(2)	125.0(4)
O(1)-C(7)-C(8)	107.6(6)	O(2)-C(7)-C(8)	127.3(6)
C(7)-C(8)-O(3)	108.6(9)	C(8)-O(3)-C(9)	119.7(10)

In principle, the synthesis of the NAMI-A like compounds incorporating **LN1** or **LN2** involves the reaction of the NAMI-A precursor, $[(\text{dmsO})_2\text{H}][\text{trans-RuCl}_4(\text{dmsO})_2]$,²⁴ with **LN1** or **LN2**. ESI-MS analysis of the residue generated from the reaction of $[(\text{dmsO})_2\text{H}][\text{trans-RuCl}_4(\text{dmsO})_2]$ with **LN2** in acetone at room temperature revealed the formation of a mixture of products. In contrast, $[\text{HLN1}][\text{trans-RuCl}_4(\text{dmsO})(\text{LN1})]$, **4**, was obtained in good yield under the same experimental conditions (Scheme 3).



Scheme 3. Synthesis of **4**, a NAMI-A like complex containing the EA skeleton.

Conductivity measurements and NMR spectroscopy were used to assess the stability of **1-4** in dmsO/H₂O mixture at 37 °C. These experiments suggest that, in the cases of **2** and **3**, rapid chloride release takes place to afford aquated, ionic species. Furthermore, the NMR spectra indicate that progressive dissociation of **LN1** from **2** (approximately 30% after 17 h and 75% after 72 h), **LN2** from **3** (38% after 17 h and *ca.* 75% after 72 h) and **LN1** from **4** (approximately 90% after 17 h, almost complete after 72 h) takes place. Complex **1** appears to be more inert toward ligands displacement, and only 20% **LP** was found not to be coordinated to the ruthenium(II) center after 72 h.

Biological studies

The ability of the compounds, except **LN1** due to solubility problems, to inhibit cell growth was evaluated against the cisplatin-sensitive A2780 and the cisplatin-resistant A2780cisR human ovarian carcinoma cell lines and non-tumoral HEK-293 (immortalized human embryonic kidney) cells (Table 2). On the two cancer cell lines all the tested ligands and complexes are considerably more cytotoxic than RAPTA-C. Even the ligands, **LP** and **LN2**, are more cytotoxic than EA-CO₂H, and there is little difference in cytotoxicity between the ligands and complexes **1 - 4**. The IC₅₀ values obtained for all the compounds are significantly lower than the corresponding ones referred to NAMI-A.¹⁹ Conversely, the IC₅₀ values of **1-4** are similar to those previously reported for ruthenium(II)-arene complexes modified with an EA-CO₂H unit, attached either via the η⁶-arene ligand or via an imidazole co-ligand.^{12,13} Based on these observations, it seems plausible that the EA-CO₂H fragment contributes to the anticancer effect via the inhibition of GSTs, which sensitizes the cancer cells towards the ruthenium fragments. Esterases may be implicated in separating the EA-CO₂H fragment from the ligand/complex.²⁰ Such a hypothesis has been proposed previously.¹⁵

Table 2. IC₅₀ values (μM) determined for RAPTA-C,²¹ EA-CO₂H, cisplatin, **LP**, **LN2** and **1 - 4** on human ovarian (A2780 and A2780cisR) cancer cells and human embryonic kidney (HEK-293) cells at 72 h. Values are given as the mean ± SD.

Compnd.	A2780	A2780cisR	HEK-293
RAPTA-C	230	270	>1000
EA-CO₂H	40 ± 3	53 ± 5	-
LP	9 ± 1	40 ± 4	38 ± 9
LN1	-	-	-
LN2	13 ± 2	11 ± 1	7.0 ± 0.5
1	11 ± 2	15 ± 4	13 ± 4
2	21 ± 2	41 ± 6	22 ± 1
3	13 ± 3	26 ± 2	16 ± 3
4	31 ± 8	27 ± 2	21 ± 3
cisplatin	0.9 ± 0.1	25 ± 3	9 ± 2
NAMI-A	>500 ¹⁹	>500 ¹⁹	>500

The compounds are not endowed with cancer cell selectivity, i.e. they are also cytotoxic to the HEK-293 cells. Complexes **1 - 3** have similar IC₅₀ values on both the A2780 and HEK-293 cells and are less active against A2780cisR cells that are cross-resistant to cisplatin. It has been shown that one mechanism of cisplatin resistance is due to over-expression of GSTs,²² which could reduce the efficacy of these complexes and an excess of EA-CO₂H would be needed to overcome resistance. In order to investigate this point, residual intracellular GST activities after incubation with complexes **1 - 4** were

determined by fluorescence spectroscopy (Figure 3). Since the 50% growth-inhibitory concentration of **1** – **4** differed between the A2780, A2780cisR and HEK cell lines (Table 2), GST activity in each cell line was measured at the IC₅₀ concentration, but over a shorted incubation period. Incubation with **1** - **4** led to a decrease in GST activity by 10 - 30% in A2780cisR cells, whereas in the other cell lines no activity decrease was observed. These results indicate that inhibition of the GSH/GST detoxification system in A2780cisR contributes to the relatively high cytotoxicities (IC₅₀ values comparable to IC₅₀ values in A2780 cells).

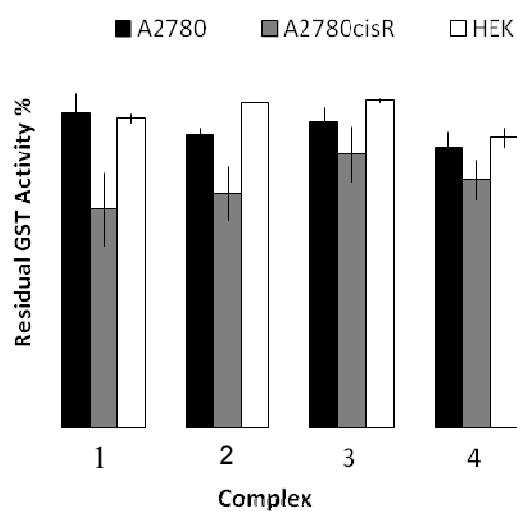


Figure 3. Residual GST activity in A2780, A2780cisR and HEK cell lines, expressed as % of control. The changes in fluorescence over a 40 min period were used to calculate GST activities.

Conclusions

Novel *P*- and *N*-donor ligands modified with ethacrynic acid were prepared and coordinated to ruthenium(II)-*p*-cymene and NAMI-like complexes. The antiproliferative activity of all of the compounds was determined, with little difference between the ligands and the complexes discerned, although all compounds are markedly more cytotoxic than RAPTA-C, NAMI-A and EA-CO₂H. The

Ru-N bond within N-donor based complexes is labile in aqueous-dmsO solutions and is expected to partially dissociate prior to cellular uptake. In contrast, the Ru-P bond is significantly more stable, and dissociation of the EA-CO₂H fragment presumably takes place following uptake of the related complex into the cell. Despite these differences, the activity of all the compounds is similar in the in vitro studies (cytotoxicity and residual GST activity), nevertheless, in vivo, the simultaneous delivery of the two active components to the tumor, i.e. the ruthenium species and the EA-CO₂H unit, is likely to be important.

Experimental

RuCl₃·3H₂O (99.9%) was purchased from Strem and the organic reactants were obtained from Alfa Aesar or Apollo Sci. and were of the highest purity available. Solvents were purchased from Sigma Aldrich. Complexes $[(\eta^6\text{-}p\text{-cymene})\text{RuCl}_2]_2$ ²³ and $[(\text{dmsO})_2\text{H}][\text{trans-RuCl}_4(\text{dmsO})_2]$ ²⁴ were prepared according to literature methods. The synthesis of **EA-(C=O)O(CH₂)₂OH**, **LP**, **LN1** and **LN2** was performed under nitrogen atmosphere using solvents distilled over P₄O₁₀. NMR spectra were recorded at 298 K on a Bruker Avance DRX400 instrument equipped with a BBFO broadband probe. The chemical shifts for ¹H and ¹³C NMR spectra were referenced to a non-deuterated aliquot of the solvent and spectra were assigned with the assistance of ¹H, ¹³C correlation spectroscopy using *gs*-HSQC and *gs*-HMBC techniques.²⁵ Infrared spectra were recorded at 298 K on a Perkin Elmer FT IR spectrometer equipped with UATR sampling accessory. Carbon, hydrogen and nitrogen analysis was performed on a Carlo Erba mod. 1106 instrument. Mass spectra were obtained on a ThermFinnigan LCQ Deca XP Plus Quadrupole ion-trap instrument in the positive ion mode. Melting points are uncorrected and were recorded on a STMP3 Stuart scientific instrument with a capillary apparatus. Conductivity measurements were carried out using an Eutech Con 700 Instrument (cell constant = 1.0 cm⁻¹).²⁶

Synthesis of 2-hydroxyethyl-2-(2,3-dichloro-4-(2-methylenebutanoyl)phenoxy)acetate, EA-C(=O)O(CH₂)₂OH

A mixture of EA-CO₂H (200 mg, 0.660 mmol) and ethylene glycol (0.15 mL, 2.69 mmol) in CH₂Cl₂ (20 mL) was treated with EDCI (127 mg, 0.662 mmol) and then with DMAP (12 mg, 0.098 mmol). The resulting mixture was allowed to stir at room temperature overnight. The resulting colorless solution was charged on a silica column. A minor fraction corresponding to EA-C(=O)O(CH₂)₂O(C=O)-EA²⁷ was collected by using CH₂Cl₂/Et₂O (3:1 v/v ratio) as eluent. Then EA-C(=O)O(CH₂)₂OH was eluted with CH₂Cl₂/Et₂O (1:1 v/v ratio). The product was isolated as a colorless powder upon removal of the solvent. Yield 171 mg, 75%. Anal. calcd. for C₁₅H₁₆Cl₂O₅: C, 51.89; H, 4.65. Found: C, 51.75; H, 4.76. Mp: 92 °C. IR (solid state): $\nu = 3511\text{m}, 2974\text{w}, 2920\text{w}, 2880\text{w}, 1736\text{s}, 1661\text{s}, 1586\text{m-s}, 1471\text{m}, 1444\text{w}, 1382\text{m}, 1357\text{w}, 1291\text{m-s}, 1257\text{m}, 1229\text{vs}, 1204\text{vs}, 1123\text{m}, 1075\text{vs}, 1012\text{m}, 1000\text{s}, 943\text{m-s}, 891\text{m}, 840\text{m}, 809\text{m}, 768\text{m}, 735\text{w cm}^{-1}$. ¹H NMR (CDCl₃): $\delta = 7.16$ (d, 1 H, ³J_{HH} = 8.48 Hz, C11-H); 6.82 (d, 1 H, ³J_{HH} = 8.48 Hz, C10-H); 5.93, 5.59 (d, 2 H, ²J_{HH} = 1.46 Hz, C4-H); 4.79 (s, 2 H, C12-H); 4.31, 3.82 (m, 4 H, C14-H + C15-H); 2.44 (q, 2 H, ³J_{HH} = 7.4 Hz, C2-H); 1.85 (m, 1 H, OH); 1.12 ppm (t, 3 H, ³J_{HH} = 7.4 Hz, C1-H). ¹³C{¹H} NMR (CDCl₃): $\delta = 195.9$ (C5); 168.0 (C13); 155.4 (C9); 150.1 (C3); 133.8 (C8); 131.4 (C7); 128.9 (C4); 126.9 (C11); 110.9 (C10); 123.2 (C6); 66.9 (C14); 66.2 (C12); 60.6 (C15); 23.4 (C2); 12.4 ppm (C1).

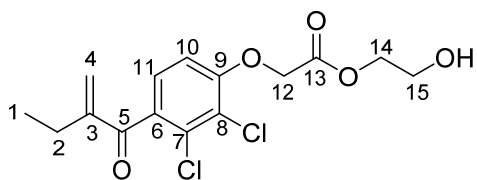


Chart 1. EA-C(=O)CH₂CH₂OH (numbering refers to carbon atoms).

Synthesis of 2-((4-(diphenylphosphanyl)benzyl)oxy)ethyl-2-(2,3-dichloro-4-(2-methylenebutanoyl)phenoxy)acetate, LP

LP was prepared by the same procedure described for the synthesis of EA-(C=O)O(CH₂)₂OH, from EA-(C=O)O(CH₂)₂OH (400 mg, 1.15 mmol), 4-(diphenylphosphino)benzoic acid (387 mg, 1.27 mmol), EDCI (220 mg, 1.15 mmol) and DMAP (20 mg, 0.164 mmol). Chromatography: hexane/Et₂O (1:4 v/v ratio). Colorless solid, yield 453 mg (62%). Anal. calcd. for C₃₄H₂₉Cl₂O₆P: C, 64.26; H, 4.60. Found: C, 64.12; H, 4.67. ESI-MS(+): *m/z* found 635.117 [M+H]⁺, calcd. for C₃₄H₃₀Cl₂O₆P⁺ 635.116; the isotopic pattern fits well the calculated one. Mp: 72-74°C. IR (solid state): *ν* = 3071w-br, 2964w-sh, 2121w-br, 1763m, 1746m-sh, 1718m-s, 1665m, 1584m, 1468w-m, 1434m, 1394w-m, 1384w-m, 1338w, 1266vs, 1193s, 1181s, 1121m, 1107m, 1080vs, 1017m, 999m, 941w-m, 895w, 850w, 802w-m, 761m-s, 743s, 718w-m, 694vs cm⁻¹. ¹H NMR (CDCl₃): δ = 7.98 (8 H, C18-H + C18'-H + C19-H + C19'-H + Ph); 7.36 (6 H, Ph); 7.09 (d, 1 H, ³J_{HH} = 8.5 Hz, C11-H); 6.82 (d, 1 H, ³J_{HH} = 8.5 Hz, C10-H); 5.93, 5.58 (m, 2 H, C4-H); 4.79 (s, 2 H, C12-H); 4.56 (m, 4 H, C14-H + C15-H); 2.47 (q, 2 H, ³J_{HH} = 7.4 Hz, C2-H); 1.15 ppm (t, 3 H, ³J_{HH} = 7.4 Hz, C1-H). ¹³C{¹H} NMR (CDCl₃): δ = 195.7 (C5); 167.6 (C13); 166.1 (C16); 155.4 (C9); 150.1 (C3); 144.8 (d, ¹J_{CP} = 14.3 Hz, P-C); 136.1 (C20); 134.0, 133.2 (d, ²J_{CP} = 19 Hz, C19 + C19'), 129.4-129.2 (C18 + C18' + Ph); 132.3 (C8); 131.5 (C7); 130.5 (C17); 128.7 (C4); 126.8 (C11); 110.9 (C10); 123.4 (C6); 66.1 (C12); 63.3, 62.4 (C14 + C15); 23.4 (C2); 12.4 ppm (C1). ³¹P NMR (CDCl₃): δ = -4.9 ppm.

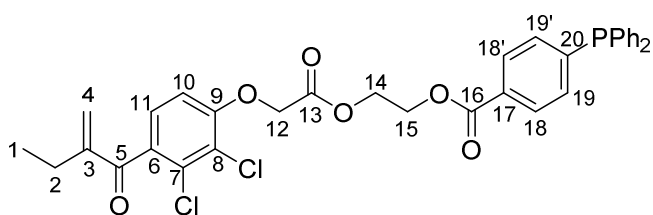


Chart 2. LP (numbering refers to carbon atoms).

Synthesis of pyridin-4-yl-methyl-2-(2,3-dichloro-4-(2-methylenebutanoyl)phenoxy)acetate, LN1

LN1 was prepared by the same procedure described for the synthesis of EA-(C=O)O(CH₂)₂OH, from EA-CO₂H (428 mg, 1.41 mmol), 4-pyridinemethanol (140 mg, 1.28 mmol), EDCI (245 mg, 1.28

mmol) and DMAP (23 mg, 0.188 mmol). Chromatography: hexane/Et₂O (progressively decreasing v/v ratio). Colorless solid stored at -30 °C, yield 430 mg (77%). Anal. calcd. for C₁₉H₁₇Cl₂NO₄: C, 57.81; H, 4.39; N, 3.21. Found: C, 57.90; H, 4.26; N, 3.12. IR (solid state): $\nu = 2969\text{w}, 2935\text{w}, 2376\text{m}, 2279\text{w}, 1762\text{s}, 1662\text{s}, 1633\text{m}, 1584\text{s}, 1508\text{w}, 1468\text{m}, 1436\text{s}, 1383\text{m}, 1293\text{m}, 1258\text{m}, 1185\text{vs}, 1168\text{vs}, 1122\text{m}, 1077\text{vs}, 1001\text{m}, 940\text{w}, 893\text{w}, 809\text{s}, 767\text{m}, 731\text{w}, 706\text{w}, 665\text{w cm}^{-1}$. ¹H NMR (CDCl₃): $\delta = 8.54$ (d, 2 H, ³J_{HH} = 4.3 Hz, C17-H + C17'-H); 7.46 (d, 2 H, ³J_{HH} = 4.6 Hz, C16-H + C16'-H); 7.13 (d, 1 H, ³J_{HH} = 8.3 Hz, C11-H); 6.83 (d, 1 H, ³J_{HH} = 8.3 Hz, C10-H); 5.95, 5.57 (m, 2 H, C4-H); 5.25 (s, 2 H, C14-H); 4.86 (s, 2 H, C12-H); 2.45 (q, 2 H, ³J_{HH} = 7 Hz, C2-H); 1.16 ppm (t, 3 H, ³J_{HH} = 7 Hz, C1-H). ¹³C{¹H} NMR (CDCl₃): $\delta = 195.6$ (C5); 167.1 (C13); 155.1 (C9); 150.1 (C3); 147.9 (C15); 147.6 (C17); 134.2 (C8); 131.6 (C7); 128.9 (C4); 126.8 (C11); 123.4 (C6); 123.3 (C16); 110.9 (C10); 66.1 (C12); 64.2 (C14); 23.4 (C2); 12.4 ppm (C1).

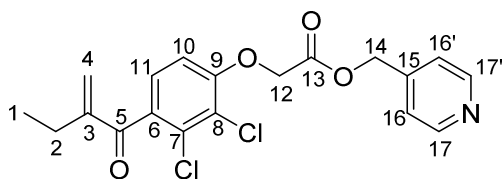


Chart 3. LN1 (numbering refers to carbon atoms).

Synthesis of 2-(2-(2,3-dichloro-4-(2-methylbutanoyl)phenoxy)acetoxymethyl)nicotinate, LN2

LN2 was prepared by the same procedure described for the synthesis of EA-(C=O)O(CH₂)₂OH, from EA-(C=O)O(CH₂)₂OH (220 mg, 0.634 mmol), nicotinic acid (94 mg, 0.761 mmol), EDCI (122 mg, 0.636 mmol) and DMAP (11 mg, 0.090 mmol). Chromatography: Et₂O. Colorless solid, yield 232 mg (81%). Anal. calcd. for C₂₁H₁₉Cl₂NO₆: C, 55.77; H, 4.23; N, 3.10. Found: C, 55.90; H, 4.35; N, 3.13. ESI-MS(+): m/z found 452.067 [M+H]⁺, calcd. for C₂₁H₂₀Cl₂NO₆⁺ 452.067; the isotopic pattern fits well the calculated one. Mp: 87-89 °C. IR (solid state): $\nu = 3063\text{w}, 2966\text{w}, 2919\text{w}, 1759\text{m}, 1731\text{m-br}, 1664\text{m}, 1583\text{s}, 1573\text{s}, 1505\text{vs}, 1483\text{vs}, 1455\text{m}, 1447\text{w-m}, 1435\text{w}, 1400\text{s}, 1386\text{vs}, 1369\text{s}, 1287\text{s}, 1269\text{s},$

1246m, 1234s, 1192vs, 1166m, 1139m, 1116m, 1079s, 1070m-sh, 1058m, 1027m, 1013vs, 996s, 975w-m, 961w, 936vs, 916w, 908w, 833s, 828w, 801m, 766m-sh, 756vs, 748vs, 699vs, 687s, 681s cm⁻¹. ¹H NMR (CDCl₃): δ = 9.23 (s, 1 H, C18-H); 8.80 (d, 1 H, ³J_{HH} = 4.89 Hz, C19-H); 8.28 (m, 1 H, C21-H); 7.43 (m, 1 H, C20-H); 7.09 (d, 1 H, ³J_{HH} = 8.5 Hz, C11-H); 6.81 (d, 1 H, ³J_{HH} = 8.5 Hz, C10-H); 5.93, 5.58 (m, 2 H, C4-H); 4.81 (s, 2 H, C12-H); 4.60 (m, 4 H, C14 + C15); 2.46 (q, 2 H, ³J_{HH} = 7.34 Hz, C2-H); 1.15 ppm (t, 3 H, ³J_{HH} = 7.34 Hz, C1-H). ¹³C{¹H} NMR (CDCl₃): δ = 195.7 (C5); 167.6 (C13); 165.0 (C16); 155.3 (C9); 153.7 (C19); 150.9 (C18); 150.1 (C3); 137.3 (C21); 134.0 (C8); 131.5 (C7); 128.6 (C4); 126.8 (C11); 125.5 (C17); 123.5 (C20); 123.4 (C6); 110.8 (C10); 66.1 (C12); 63.1, 62.8 (C14, C15); 23.4 (C2); 12.4 ppm (C1).

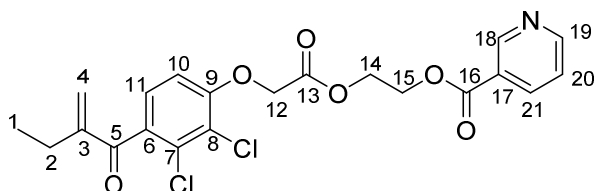


Chart 4. LN2 (numbering refers to carbon atoms).

Synthesis of Ru(η^6 -*p*-cymene)Cl₂(2-((4-(diphenylphosphanyl)benzyl)oxy)ethyl-2-(2,3-dichloro-4-(2-methylenebutanoyl)phenoxy)acetate), **1**.

[Ru(η^6 -*p*-cymene)Cl₂]₂ (0.140 g, 0.229 mmol) was added to a solution of **LP** (330 mg, 0.519 mmol) in CHCl₃ (20 mL). The resulting mixture was heated at reflux for 18 h. The resulting red solution was cooled to room temperature and the solvent was removed under reduced pressure. The dark-red residue was washed with Et₂O (3 x 20 mL) and then dried under vacuum. The product, **1**, was obtained as a dark-red solid. Yield 256 mg, 60%. **1** is soluble in chlorinated solvents and dmsO and insoluble in H₂O. Anal. calcd. for C₄₄H₄₃Cl₄O₆PRu: C, 56.12; H, 4.60. Found: C, 56.24; H, 4.73. ESI-MS(+): *m/z* found 906.091 [M-Cl]⁺, calcd. for C₄₄H₄₃Cl₃O₆PRu⁺ 906.098; the isotopic pattern fits well the calculated one. Mp: 117-118 °C. IR (solid state) *v*: 3058w-br, 2965w-m-sh, 1760m, 1717m-s, 1663m, 1584m, 1469m,

1435m, 1384m, 1338w, 1263s, 1187s, 1110m-s, 1079vs, 1017m-s, 1000m, 942w-m, 895w-m, 854w-m, 800m, 762m, 748m, 721m, 696vs cm^{-1} . ^1H NMR (CDCl_3): $\delta = 7.93, 7.84, 7.43$ (14 H, C18-H + C18'-H + C19-H + C19'-H + Ph); 7.11 (m, 1 H, C11-H); 6.82 (m, 1 H, C10-H); 5.94, 5.60 (m, 2 H, C4-H); 5.25, 5.00 (m, 4 H, arom $\text{CH}_{\text{cymene}}$); 4.79 (s, 2 H, C12-H); 4.53 (m, 4 H, C14-H + C15-H); 2.88 (m, 1 H, CHMe_2); 2.46 (m, 2 H, C2-H); 1.88 (s, 3 H, MeC_6H_4); 1.35-1.13 ppm (m, 9 H, C1-H + CHMe_2). $^{13}\text{C}\{^1\text{H}\}$ NMR (CDCl_3): $\delta = 195.8$ (C5); 167.5 (C13); 165.8 (C16); 155.3 (C9); 150.1 (C3); 139.8, 139.3, 136.7 (C20 + P-C); 134.5, 134.4, 128.7, 128.3 (C18 + C18' + C19 + C19' + arom CH_{Ph}); 133.3 (C8); 131.5 (C7); 132.4 (C17); 129.5 (C4); 126.9 (C11); 111.0 (C10); 123.3 (C6); 111.6 (CCHMe_2); 96.3 (arom CMe); 88.8, 87.4 (arom $\text{CH}_{\text{cymene}}$); 66.0 (C12); 63.2, 62.3 (C14 + C15); 30.3 (CHMe_2); 23.4 (C2); 21.8 (CHMe_2); 17.8 (MeC_6H_4); 12.4 ppm (C1). ^{31}P NMR (CDCl_3): $\delta = 25.3$ ppm.

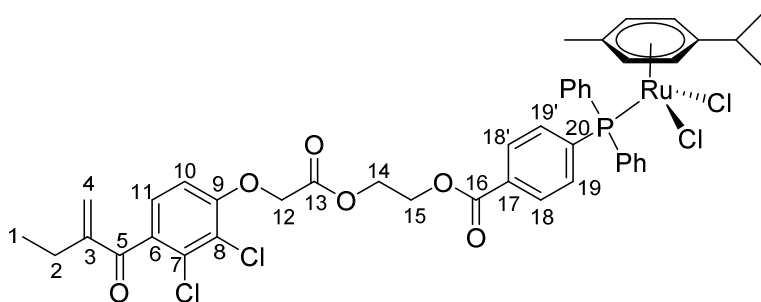


Chart 5. $\text{Ru}(\eta^6\text{-}p\text{-cymene})\text{Cl}_2(\text{LP})$, **1** (numbering refers to carbon atoms).

Synthesis of $\text{Ru}(\eta^6\text{-}p\text{-cymene})\text{Cl}_2(\text{pyridin-4-yl-methyl-2-(2,3-dichloro-4-(2-ethylnebutanoyl)phenoxy)acetate})$, **2**

$[\text{Ru}(\eta^6\text{-}p\text{-cymene})\text{Cl}_2]_2$ (0.120 g, 0.196 mmol) was added to a solution of **LN1** (185 mg, 0.469 mmol) in CH_2Cl_2 (20 mL). The resulting mixture was allowed to stir at room temperature for 18 h and the solvent was removed under reduced pressure. CHCl_3 (2 mL) and then of Et_2O (50 mL) were added. The resulting precipitate was washed with Et_2O (2 x 20 mL) and then dried under vacuum. The product, **2**, was obtained as a red solid. Yield 203 mg, 74%. Red crystals suitable for X-ray analysis were collected from a THF/hexane mixture settled aside at $-30\text{ }^\circ\text{C}$ for two weeks. **2** is soluble in

chlorinated solvents and dmso and insoluble in H₂O. Anal. calcd. for C₂₉H₃₁Cl₄NO₄Ru: C, 49.73; H, 4.46; N, 2.00. Found: C, 49.85; H, 4.55; N, 1.92. ESI-MS(+): *m/z* found 665.045 [M-Cl]⁺, calcd. for C₂₉H₃₁Cl₃NO₄Ru⁺ 665.044; the isotopic pattern fits well the calculated one. Mp: 166–168 °C. IR (solid state): *v* = 3075w, 2966w, 2935w, 2874w, 1764vs, 1692w, 1661m, 1616w, 1584s, 1499w, 1470m, 1446m, 1426m, 1390m, 1383m, 1364w, 1338w, 1328w, 1301m, 1244s, 1228m, 1191vs, 1120w, 1074vs, 1065vs, 1030m, 999m, 959w, 878w, 813s, 760w, 734w, 716w, 666w cm⁻¹. ¹H NMR (CDCl₃): δ = 8.88 (d, 2 H, ³J_{HH} = 5 Hz, C17-H + C17'-H); 7.16 (d, 2 H, ³J_{HH} = 5 Hz, C16-H + C16'-H); 7.06 (d, 1 H, ³J_{HH} = 8 Hz, C11-H); 6.84 (d, 1 H, ³J_{HH} = 8 Hz, C10-H); 5.88, 5.52 (m, 2 H, C4-H); 5.38, 5.17 (d, 4 H, ³J_{HH} = 5 Hz, arom CH_{cymene}); 5.14 (s, 2 H, C14-H); 4.84 (s, 2 H, C12-H); 2.87 (m, 1 H, CHMe₂); 2.38 (q, 2 H, ³J_{HH} = 7.2 Hz, C2-H); 2.00 (s, 3 H, MeC₆H₄); 1.22 (d, 6 H, ³J_{HH} = 6.8 Hz, CHMe₂); 1.06 (t, 3 H, ³J_{HH} = 7.4 Hz, C1-H) ppm. ¹³C NMR (CDCl₃): δ = 195.7 (C5); 167.2 (C13); 155.1 (C9); 154.8 (C17 + C17'); 149.9 (C3); 146.4 (C15); 133.8 (C8); 131.1 (C7); 129.0 (C4); 127.1 (C11); 122.9 (C6); 122.6 (C16 + C16'); 111.3 (C10); 103.3 (CCHMe₂); 97.2 (arom CMe); 88.8, 82.1 (arom CH_{cymene}); 66.2 (C12); 64.2 (C14); 30.6 (CHMe₂); 23.3 (C2); 22.2 (CHMe₂); 18.2 (MeC₆H₄); 12.4 (C1) ppm.

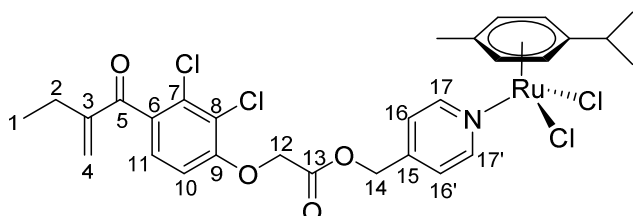


Chart 6. (η⁶-*p*-cymene)RuCl₂(LN1), **2** (numbering refers to carbon atoms).

Synthesis of Ru(η⁶-*p*-cymene)Cl₂(2-(2-(2,3-dichloro-4-(2-methylenebutanoyl)phenoxy)acetoxy)ethyl nicotinate), **3**

This compound was prepared by the same procedure described for the synthesis of **2**, from [(η⁶-*p*-cymene)RuCl₂]₂ (0.105 g, 0.171 mmol) and LN2 (185 mg, 0.409 mmol). Dark-orange solid, yield 200 mg (77%). **3** is soluble in chlorinated solvents and dmso and insoluble in H₂O. Anal. calcd. for

$C_{31}H_{33}Cl_4NO_6Ru$: C, 49.09; H, 4.39; N, 1.85. Found: C, 48.95; H, 4.39; N, 1.88. ESI-MS(+): m/z found 723.042 $[M-Cl]^+$, calcd. for $C_{31}H_{33}Cl_3NO_6Ru^+$ 723.049; the isotopic pattern fits well the calculated one. Mp: 69-70 °C. IR (solid state): $\nu = 3071w$ -br, 2963w, 2930w, 2874w, 1760m-sh, 1729s, 1662m, 1604w, 1585s, 1501w, 1469m, 1434m, 1408w, 1384m, 1363w, 1286vs, 1259s, 1195vs, 1138m, 1115s, 1079vs, 1056vs, 1031s, 1003s, 941w-br, 913w, 895w, 872w-br, 803s, 769w, 744s, 728s, 689m cm^{-1} . 1H NMR ($CDCl_3$): $\delta = 9.59$ (s, 1 H, C18-H); 9.23 (d, 1 H, $^3J_{HH} = 4.89$ Hz, C19-H); 8.30 (d, 1 H, $^3J_{HH} = 7.34$ Hz, C21-H); 7.45 (m, 1 H, C20-H); 7.12 (d, 1 H, $^3J_{HH} = 8.5$ Hz, C11-H); 6.94 (d, 2 H, $^3J_{HH} = 8.5$ Hz, C10-H); 5.93, 5.58 (s, 2 H, C4-H); 5.49, 5.30 (d, 4 H, $^3J_{HH} = 5.38$ Hz, arom CH_{cymene}); 4.95 (s, 2 H, C12-H); 4.60 (m, 4 H, C14 + C15); 2.94 (m, 1 H, $CHMe_2$); 2.45 (q, 2 H, $^3J_{HH} = 7.82$ Hz, C2-H); 2.07 (s, 3 H, MeC_6H_4); 1.30 (d, 6 H, $^3J_{HH} = 6.85$ Hz, $CHMe_2$); 1.14 ppm (t, 3 H, $^3J_{HH} = 7.82$ Hz, C1-H). $^{13}C\{^1H\}$ NMR ($CDCl_3$): $\delta = 195.8$ (C5); 167.9 (C13); 163.3 (C16); 158.3 (C19); 156.1 (C18); 155.3 (C9); 150.1 (C3); 138.9 (C21); 133.8 (C8); 131.3 (C7); 128.9 (C4); 126.7 (C11); 111.1 (C10); 127.1 (C17); 124.4 (C20); 123.0 (C6); 111.6 ($CCHMe_2$); 97.5 (arom CMe); 83.1, 82.1 (arom CH_{cymene}); 66.2 (C12); 63.4, 62.6 (C14, C15); 30.8 ($CHMe_2$); 23.4 (C2); 22.3 ($CHMe_2$); 18.3 (MeC_6H_4); 12.4 ppm (C1).

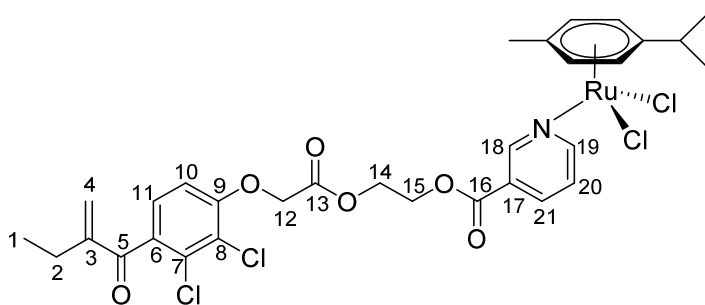


Chart 7. $(\eta^6$ -*p*-cymene) $RuCl_2(LN2)$, **3** (numbering refers to carbon atoms).

Synthesis of $[HLN1]^+[trans-RuCl_4(dmsO)(LN1)]^-$, **4**

LN1 (760 mg, 1.93 mmol) was added to a suspension of freshly prepared $[(dmsO)_2H][trans-RuCl_4(dmsO)_2]$ (505 g, 0.908 mmol) in acetone (20 mL). The mixture was stirred at room temperature,

in the dark. After 2 hours an orange solution had formed. The solvent was removed under reduced pressure and the resulting solid residue was washed with Et₂O (3 x 20 mL) and then dried under vacuum. Compound **4** was obtained as an orange microcrystalline powder. Yield 836 mg, 83%. **4** is soluble in dmsO and methanol and insoluble in H₂O. Anal. calcd. for C₄₀H₄₁Cl₈N₂O₉RuS: C, 43.26; H, 3.72; N, 2.52. Found: C, 43.11; H, 3.89; N, 2.38. ESI-MS(+): *m/z* found 394.061 [M_{HILNI}]⁺, calcd. for C₁₉H₁₈Cl₂NO₄⁺ 394.061; the isotopic pattern fits well the calculated one. ESI-MS(-): *m/z* found 715.858 [M_[trans-RuCl4(dmso)(LNI)]]⁻, calcd. for C₂₁H₂₃Cl₆NO₅RuS⁻ 715.248; the isotopic pattern fits well the calculated one. Mp: decomp. at 85 °C. IR (solid state): ν = 3210w, 3068w, 2968w, 2933w, 2870w, 1759m, 1691w, 1662m, 1643w, 1620w, 1583s, 1507w, 1468m, 1428m, 1383m, 1340w, 1293m, 1256m, 1221m, 1185vs, 1117m, 1074vs, 1020s, 1001s, 938w, 907w, 892w, 806s, 768m, 721w, 684w cm⁻¹.

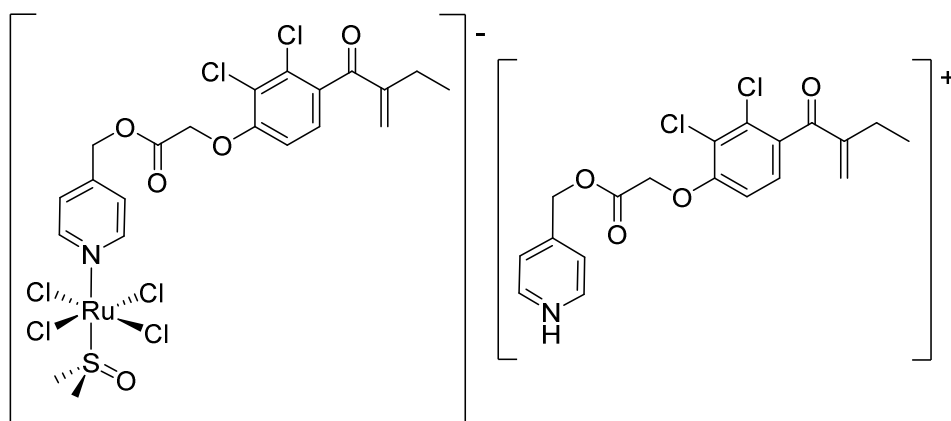


Chart 8. NAMI-A like complex containing EA.

Stability studies

A) NMR spectroscopy. *General procedure:* Complexes **1 – 4** (0.050 mmol) were dissolved in 0.55 mL of dmsO-d₆/H₂O mixture (*v/v* ratio 9:1) and CDCl₃ (0.50 mmol) was added as a reference. The NMR tubes were sealed, maintained at 37 °C and analyzed by NMR spectroscopy as a function of time. **B)**

Conductivity. *General procedure:* Complexes **1 – 3** (ca. 0.05 mmol) were dissolved in 5 mL of

DMSO/H₂O mixture (v/v ratio 9:1) and kept at 37 °C. Measurements were recorded as a function of time. *Complex 1*: 3 min, $\Lambda_M = 0.30 \text{ S}\times\text{cm}^2\times\text{mol}^{-1}$; 90 min, $\Lambda_M = 0.40 \text{ S}\times\text{cm}^2\times\text{mol}^{-1}$; 72 h, $\Lambda_M = 0.83 \text{ S}\times\text{cm}^2\times\text{mol}^{-1}$. *Complex 2*: 3 min, $\Lambda_M = 4.3 \text{ S}\times\text{cm}^2\times\text{mol}^{-1}$; 90 min, $\Lambda_M = 5.9 \text{ S}\times\text{cm}^2\times\text{mol}^{-1}$; 72 h, $\Lambda_M = 6.2 \text{ S}\times\text{cm}^2\times\text{mol}^{-1}$. *Complex 3*: 3 min, $\Lambda_M = 1.5 \text{ S}\times\text{cm}^2\times\text{mol}^{-1}$; 90 min, $\Lambda_M = 2.5 \text{ S}\times\text{cm}^2\times\text{mol}^{-1}$; 72 h, $\Lambda_M = 2.9 \text{ S}\times\text{cm}^2\times\text{mol}^{-1}$.

X-ray crystallography

Crystal data and collection details for **2**·thf are reported in Table 3. Data were recorded on a Bruker APEX II diffractometer equipped with a CCD detector using Mo–K α radiation. Data were corrected for Lorentz polarization and absorption effects (empirical absorption correction SADABS).²⁸ The structure was solved by direct methods and refined by full-matrix least-squares based on all data using F^2 .²⁹ Hydrogen atoms were fixed at calculated positions and refined by a riding model. All non-hydrogen atoms in **2** were refined with anisotropic displacement parameters, whereas the disordered thf molecule was treated isotropically. Part of the **LN1** ligand and the isopropyl group of *p*-cymene in **2** and the thf molecule are disordered and, therefore, have been split into two positions and refined isotropically using one occupancy parameter per disordered group. Similar *U* restraints were applied to the C, N and O-atoms of the **LN1** and *p*-cymene ligands (SIMU line in SHELXL, s.u. 0.01). Some atoms of the disordered groups have been restrained to isotropic behavior (ISOR line in SHELXL, s.u. 0.02). The disordered groups have been restrained to have similar geometries (SAME line in SHELXL, s.u. 0.02). The Ph-rings of the disordered **LN1** ligand were constrained to fit regular hexagons (AFIX 66 line in SHELXL). Restraints to bond distances were applied as follow (s.u. 0.02): 1.43 Å for C–O and 1.53 Å for C–C in thf.

Table 3. Crystal data and measurement details for **2**·thf.

Formula	C ₃₃ H ₃₉ Cl ₄ NO ₅ Ru
FW	772.52
T, K	293(2)
λ , Å	0.71073
Crystal system	Monoclinic
Space group	<i>P</i> 2 ₁ / <i>c</i>
<i>a</i> , Å	14.2454(11)
<i>b</i> , Å	10.6848(8)
<i>c</i> , Å	23.3046(18)
β , °	98.5820(10)
Cell Volume, Å ³	3507.5(5)
Z	4
<i>D_c</i> , g·cm ⁻³	1.463
μ , mm ⁻¹	0.791
F(000)	1584
Crystal size, mm	0.21 x 0.16 x 0.12
θ λιμιτσ, °	1.45 - 27.00
Reflections collected	37831
Independent reflections	7469 [<i>R</i> _{int} = 0.0290]
Data / restraints / parameters	7469 / 834 / 506
Goodness on fit on F ²	1.039
<i>R</i> ₁ (<i>I</i> > 2σ(<i>I</i>))	0.02479
<i>wR</i> ₂ (all data)	0.1574
Largest diff. peak and hole, e Å ⁻³	0.958 / -0.610

Cell culture

Human A2780 and A2780cisR ovarian carcinoma cells were obtained from the European Centre of Cell Cultures (ECACC, UK). Nontumorigenic HEK-293 cells were provided by the Institute of Pathology, CHUV, Lausanne, Switzerland. A2780 and A2780cisR were routinely grown in RPMI 1640 medium supplemented with GlutaMAX (Gibco), while HEK-293 were grown in DMEM medium, both containing heat-inactivated fetal calf serum (FCS, Sigma, USA) (10%) and antibiotics (penicillin/streptomycin, 1%) at 37 °C and CO₂ (5%).

Determination of antiproliferative activity

Cytotoxicity was determined using the MTT assay (MTT = 3-(4,5-dimethyl-2-thiazolyl)-2,5-diphenyl-2H-tetrazolium bromide). Cells were seeded in 96-well plates as monolayers with 100 µL of cell solution per well and pre-incubated for 24 h in the cell medium. Compounds were prepared as DMSO solutions that were rapidly dissolved in the culture medium and serially diluted to the appropriate concentration to give a final DMSO concentration of 0.5%. 100 µL of the drug solution was added to each well and the plates were incubated for another 72 h. Subsequently, MTT (5 mg/mL solution) was added to the cells and the plates were incubated for further 4 h. The culture medium was aspirated, and the purple formazan crystals formed by the mitochondrial dehydrogenase activity of vital cells were dissolved in DMSO. The optical density, directly proportional to the number of surviving cells, was quantified at 540 nm using a multiwell plate reader and the fraction of surviving cells was calculated from the absorbance of untreated control cells. Evaluation is based on means from two independent experiments, each comprising three microcultures per concentration level.

GST activity assay

A2780, A2780cisR and HEK cells were plated in six well plates and incubated for 24 h in a CO₂ incubator at 37°C. The cells were then exposed to compounds **1** – **4** at final concentrations ranging

from 10 to 40 μM , according to the IC_{50} concentration for each respective cell line, for 6 h. The cells were then washed with ice-cold PBS, harvested, lysed by a repetitive freeze-thaw cycle and centrifuged at 10,000g for 15 min at 4 °C. The supernatants were used for the analysis of GST activity according to a fluorometric GST detection kit (Abnova). The changes in fluorescent intensities at Ex/Em 380/460 nm were recorded in a kinetic mode, every 5min over 60min, on a microplate reader (Molecular Devices). The GST activities were measured in duplicate and expressed as U/min/mL per mg protein and then converted to % of control.

The GST activity of the test samples was calculated by applying the equation $\Delta\text{RFU} = \text{RFU}_2 - \text{RFU}_1$ to the GST standard curve to get B [mU] during the reaction time ($\Delta\text{T} = \text{T}_2 - \text{T}_1$). The sample GST activity is calculated by the following formula: Sample GST Activity = $B / (\Delta\text{T} \times V) \times \text{dilution factor}$ [mU/min/mL], where B is sample GST activity from the GST standard curve [mU], ΔT is the reaction time (min), V is the sample volume added into the reaction well [mL].

Protein determination

The protein concentration was determined by a Bradford assay (Bio-Rad) using BSA as a standard.

Corresponding Authors

*E-mail addresses: paul.dyson@epfl.ch, fabio.marchetti1974@unipi.it.

Notes

The authors declare no competing financial interest.

Acknowledgements

We thank the Swiss National Science Foundation and the University of Pisa for financial support.

Supporting Information Available

CCDC reference number 1056723 (2) contains the supplementary crystallographic data for the X-ray study reported in this paper. These data can be obtained free of charge at www.ccdc.cam.ac.uk/conts/retrieving.html (or from the Cambridge Crystallographic Data Centre, 12, Union Road, Cambridge CB2 1EZ, UK; fax: (internat.) +44-1223/336-033; e-mail: deposit@ccdc.cam.ac.uk).

References

-
- 1 a) van Rijjt, S. H.; Sadler, P. J. *Drug Disc. Today*, **2009**, *14*, 1089-1097. b) Gasser, G.; Ott, I.; Metzler-Nolte, N. *J. Med. Chem.* **2011**, *54*, 3-25. c) Ronconi, L.; Sadler, P. J. *Coord. Chem. Rev.* **2007**, *251*, 1633-1648. d) Barry, N. P. E.; Sadler, P. J. *Chem Commun*, **2013**, *49*, 5016-5041.
 - 2 a) Bergamo, A.; Sava, G. *Dalton Trans.*, **2007**, 1267-1272. b) Rademaker-Lakhai, J. M.; Van Den Bongard, D.; Pluim, D.; Beijnen, J. H.; Schellens, J. H. M. *Clin. Cancer Res.*, **2004**, *10*, 3717-3727. c) Hartinger, C. G.; Zorbas-Seifried, S.; Jakupec, M. A.; Kynast, B.; Zorbas, H.; Keppler, B. K. *J. Inorg. Biochem.*, **2006**, *100*, 891-904. d) Hartinger, C. G.; Jakupec, M. A.; Zorbas-Seifried, S.; Groessl, M.; Egger, A.; Berger, W.; Zorbas, H.; Dyson, P. J.; Keppler, B. K. *Chem. Biodiversity*, **2008**, *5*, 2140-2155. e) Trondl, R.; Heffeter, P.; Kowol, C. R.; Jakupec, M. A.; Berger, W.; Keppler, B. K. *Chem. Sci.*, **2014**, *5*, 2925-2932.
 - 3 a) Bratsos, I.; Gianferrara, T.; Alessio, E.; Hartinger, C. G.; Jakupec, M. A.; Keppler, B. K. in *Bioinorganic Medicinal Chemistry*, ed. E. Alessio, Wiley-VCH, Weinheim, **2011**, 151-174. b) Clarke, M. J. *Coord. Chem. Rev.* **2003**, *236*, 209-233. c) Webb, M. I.; Chard, R. A.; Al-Jobory, Y. M.; Jones, M. R.; Wong, E. W. Y.; Walsby, C. J. *Inorg. Chem.*, **2012**, *51*, 954-966.

-
- 4 a) Peacock, A. F. A.; Sadler, P. J. *Chem. Asian J.*, **2008**, *3*, 1890-1899. b) Hartinger, C. G.; Dyson, P. J. *Chem. Soc. Rev.*, **2009**, *38*, 391-401. c) Cuesta, L.; Sessler, J. L. *Chem. Soc. Rev.*, **2009**, *38*, 2716-2729. d) Suss-Fink, G. *Dalton Trans.*, **2010**, *39*, 1673-1688.
- 5 Scolaro, A. Bergamo, L. Brescacin, R. Delfino, M. Cocchietto, G. Laurency, T. J. Geldbach, G. Sava, P. J. Dyson, *J. Med. Chem.*, **2005**, *48*, 4161-4171. b) Bergamo, A. Masi, P. J. Dyson, G. Sava, *Int. J. Onco.*, **2008**, *33*, 1281-1289. c) Weiss, A.; Berndsen, R. H.; Dubois, M.; Müller, C.; Schibli, R.; Griffioen, A. W.; Dyson, P. J.; Nowak-Sliwinska, P. *Chem. Sci.*, **2014**, *5*, 4742 – 4748.
- 6 a) Chari, R. V. J.; Miller, M. L.; Widdison, W. C. *Angew. Chem. Int. Ed.* **2014**, *53*, 3796-3827. b) Hanifa, M.; Meier, S. M.; Kandioller, W.; Bytzeck, A.; Hejl, M.; Hartinger, C. G.; Nazarov, A. A.; Arion, V. B.; Jakupec, M. A.; Dyson, P. J.; Keppler, B. K. *J. Inorg. Biochem.* **2011**, *105*, 224-231. c) N. Margiotta, N. Denora, R. Ostuni, V. Laquintana, A. Anderson, S. W. Johnson, G. Trapani, G. Natile, *J. Med. Chem.* **2010**, *53*, 5144-5154.
- 7 a) Nazarov, A. A.; Hartinger, C. G.; Dyson, P. J. *J. Organomet. Chem.*, **2014**, *751*, 251-260. b) Singh, A. K.; Pandey, D. S.; Xu, Q.; Braunstein, P. *Coord. Chem. Rev.*, **2014**, *270-271*, 31-56. c) Hartinger, C. G.; Phillips, A. D.; Nazarov, A. A. *Curr. Top. Med. Chem.*, **2011**, *11*, 2688-2702. d) Levina, A.; Mitra, A.; Lay, P.A. *Metallomics*, **2009**, *1*, 458-470. e) Gasser, G.; Ott, I.; Metzler-Nolte, N. *J. Med. Chem.*, **2011**, *54*, 3-25.
- 8 a) Kurzwernhart, A.; Kandioller, W.; Bächler, S.; Bartel, C.; Martic, S.; Buczkowska, M.; Mühlgassner, G.; Jakupec, M. A.; Kraatz, H.-B.; Bednarski, P. J. *J. Med. Chem.*, **2012**, *55*, 10512-10522. b) Kurzwernhart, A.; Kandioller, W.; Bartel, C.; Bächler, S.; Trondl, R.; Mühlgassner, G.; Jakupec, M. A.; Arion, V. B.; Marko, D.; Keppler, B. K. *Chem. Commun.*, **2012**, *48*, 4839-4841. c) Kurzwernhart, A.; Kandioller, W.; Enyedy, É. A.; Novak, M.; Jakupec, M. A.; Keppler, B. K.; Hartinger, C. G. *Dalton Trans.*, **2013**, *42*, 6193-6202.

-
- 9 Kandioller, W.; Balsano, E.; Meier, S. M.; Jungwirth, U.; Goschl, S.; Roller, A.; Jakupec, M. A.; Berger, W.; Keppler, B. K.; Hartinger, C. G. *Chem. Commun.*, **2013**, *49*, 3348-3350.
- 10 Arion, V. B.; Dobrov, A.; Goschl, S.; Jakupec, M. A.; Keppler, B. K.; *Chem. Commun.*, **2012**, *48*, 8559-8561.
- 11 Nazarov, A. A.; Meier, S. M.; Zava, O.; Nosova, Y. N.; Milaeva, E. R.; Hartinger, C. G.; Dyson, P. *J. Dalton Trans.*, **2015**, *44*, 3614-23.
- 12 Ang, W. H.; Parker, L. J.; De Luca, A.; Juillerat-Jeanneret, L.; Morton, C. J.; Lo Bello, M.; Parker, M. W.; Dyson, P. J. *Angew. Chem. Int. Ed.* **2009**, *48*, 3854-3857.
- 13 Ang, W. H.; De Luca, A.; Chapuis-Bernasconi, C.; Juillerat-Jeanneret, L.; Lo Bello, M.; Dyson, P. *J. ChemMedChem*, **2007**, *2*, 1799-1806.
- 14 a) Ang, W. H.; Khalaila, I.; Allardyce, C. S.; Juillerat-Jeanneret, L.; Dyson, P. J. *J. Am. Chem. Soc.*, **2005**, *127*, 1382-1383. b) Parker, L. J.; Italiano, L. C.; Morton, C. J.; Hancock, N. C.; Ascher, D. B.; Aitken, J. B.; Harris, H. H.; Campomanes, P.; Rothlisberger, U.; De Luca, A.; Lo Bello, M.; Ang, W.-H.; Dyson, P. J.; Parker, M. W. *Chem. Eur. J.*, **2011**, *17*, 7806-7816.
- 15 a) Chatterjee, S.; Biondi, I.; Dyson, P. J.; Bhattacharyya, A.; *J. Biol. Inorg. Chem.*, **2011**, *16*, 715-724. b) Johansson, K.; Ito, M.; Schopuizen, C. M. S.; Thengumtharayil, S. M.; Heuser, V. D.; Zhang, J.; Shimoji, M.; Vahter, M.; Ang, W. H.; Dyson, P. J.; Shibata, A.; Shuto, S.; Ito, Y.; Abe, H.; Morgenstern, R. *Mol. Pharmaceutics*, **2011**, *8*, 1698-1708.
- 16 a) Wang, Z.; Qian, H.; Yiu, S.-M.; Sun, J.; Zhu, G. *J. Inorg. Biochem.* **2014**, *131*, 47-55. b) Grgurić-Sípka, S.; Ivanović, I.; Rakić, G.; Todorović, N.; Gligorijević, N.; Radulović, S.; Arion, V. B.; Keppler, B. K.; Tešić, Z. Lj. *Eur. J. Med. Chem.* **2010**, *45*, 1051-1058. c) Sáez, R.; Lorenzo, J.; Prieto, M. J.; Font Bardia, M.; Calvet, T.; Omeñaca, N.; Vilaseca, M.; Moreno, V. *J. Inorg. Biochem.*, **2014**, *136*, 1-12. d) Clavel, C. M.; Paunescu, E.; Nowak-Sliwinska, P.; Griffioen, A. W.; Scopelliti, R.; Dyson, P. J.; *J. Med. Chem.* **2014**, *57*, 3546-3558.

-
- 17 a) Allardyce, C. S.; Dyson, P. J.; Ellis, D. J.; Heath, S. L. *Chem. Commun.* **2001**, 1396-1397. b) Morris, R.E.; Aird, R.E.; del S. Murdoch, P.; Chen, H.; Cummings, J.; Hughes, N.D.; Parsons, S.; Parkin, A.; Boyd, G.; Jodrell, D.I.; Sadler, P. J. *J. Med. Chem.* **2001**, *44*, 3616-3621. c) Vock, C. A.; Scolaro, C.; Phillips, A. D.; Scopelliti, R.; Sava, G.; Dyson, P. J. *J. Med. Chem.* **2006**, *49*, 5552-5561.
- 18 Lamotre, P. J.; Campsteyn, H.; Dupont, L.; Vermeire, M. *Acta Cryst.*, **1978**, *B34*, 2636-2638.
- 19 a) Casini, A.; Edafe, F.; Erlandsson, M.; Gonsalvi, L.; Ciancetta, A.; Re, N.; Ienco, A.; Messori, L.; Peruzzini, M.; Dyson, P. J. *Dalton Trans.*, **2010**, *39*, 5556-5563. b) Groessl, M.; Zava, O.; Dyson, P. J. *Metallomics*, **2011**, *3*, 591-599.
- 20 Cynkowska, G.; Cynkowski, T.; Al-Ghananeem, A. A.; Guo, H.; Ashton, P.; Crooks, P. A. *Bioorg. Med. Chem. Lett.*, **2005**, *15*, 3524-3527.
- 21 Kilpin, K. J.; Clavel, C. M.; Edafe, F.; Dyson, P. J. *Organometallics*, **2012**, *31*, 7031-7039.
- 22 Johansson, K.; Ito, M.; Schophuizen, C. M. S.; Thengumtharayil, S. M.; Heuser, V. D.; Zhang, J.; Shimoji, M.; Vahter, M.; Ang, W. H.; Dyson, P. J.; Shibata, A.; Shuto, S.; Ito, Y.; Abe, H.; Morgenstern, R. *Mol. Pharmaceutics*, **2011**, *8*, 1698-1708.
- 23 Bennett, M. A.; Smith, A. K. *J. Chem. Soc. Dalton Trans.* **1974**, 233-241.
- 24 Li, L.; Wong, Y.-S.; Chen, T.; Fana, C.; Zheng, W. *Dalton Trans.* **2012**, *41*, 1138-1141.
- 25 Willker, W.; Leibfritz, D.; Kerssebaum, R.; Bermel, W. *Magn. Reson. Chem.* **1993**, *31*, 287-292.
- 26 a) Jutand, A. *Eur. J. Inorg. Chem.*, **2003**, 2017-2040. b) Geary, W. J. *Coord. Chem. Rev.*, **1971**, *7*, 81-122.
- 27 Yield 21 mg, 10%. Anal. Calcd. for C₂₉H₂₉Cl₄O₈: C, 53.81; H, 4.52. Found: C, 53.67; H, 4.57. ¹H NMR (CDCl₃): δ = 7.17, 6.82 (d, 4 H, ³J_{HH} = 8.48 Hz); 5.96, 5.62 (d, 4 H, ²J_{HH} = 1.17 Hz); 4.79 (s, 4 H); 4.49 (s, 4 H); 2.50 (q, 2 H, ³J_{HH} = 7.4 Hz); 1.17 ppm (t, 3 H, ³J_{HH} = 7.4 Hz). ¹³C{¹H} NMR

(CDCl₃): δ = 195.8, 167.6, 155.3, 150.1, 134.1, 131.5, 128.8, 126.8, 110.9, 123.4, 66.0, 62.9, 23.4, 12.4 ppm.

28 Sheldrick, G. M. SADABS, Program for empirical absorption correction, University of Göttingen, Germany, **1996**.

29 Sheldrick, G. M. SHELX97, Program for crystal structure determination, University of Göttingen, Germany, **1997**.

Table of Contents Synopsis and graphic

Novel ruthenium(II) and ruthenium(III) complexes with ethacrynic acid-modified ligands were prepared and their antiproliferative activity was determined.

